Comparison of Localized Hyperpolarized ^{13}C-Pyruvate and ^{13}C-Urea Dynamics in Tumor Models

Peder E. Z. Larson[1], Kayvan R Keshari[2], David M Wilson[2], Simon Hu[2], Michael Lustig[3], Adam B Kerr[4], John M Pauly[4], John Kurhanewicz[2], and Daniel B Vigneron[2]
[1]UCSF, San Francisco, California, United States, [2]UCSF, [3]UC Berkeley, [4]Stanford University

Introduction: Time-resolved MR spectroscopic imaging (MRSI) following injection of hyperpolarized [1-^{13}C]-pyruvate can provide valuable and detailed metabolic information, including perfusion, uptake and kinetics, and has been shown in a murine prostate tumor model to improve distinction and characterization of cancerous tissue [1]. Interpreting metabolic information can be confounded by perfusion of [1-^{13}C]-lactate produced outsize the tissue of interest. In this study, copolarization [2] and simultaneous injection of [1-^{13}C]-pyruvate (metabolic marker) and ^{13}C-urea (perfusion marker) [3] was combined with a dynamic 3D EPSI acquisition to better characterize perfusion and uptake of hyperpolarized agents, and allow for distinction of perfusion versus tissue metabolic conversion.

Methods: We used a 3D hyperpolarized ^{13}C dynamic MRSI acquisition with multiband excitation pulses and a compressed sensing acquisition and reconstruction [4]. The multiband excitation pulse was modified to include an excitation band for ^{13}C-urea, with flip angles of 6-degrees for [1-^{13}C]-pyruvate and ^{13}C-urea, and 12-degrees for [1-^{13}C]-lactate and [1-^{13}C]-alanine. The pulse had a 6 cm minimum slice thickness for a 4 G/cm maximum gradient strength. The acquisition was started after completion of the injection and minimal spin-echo crusher gradient amplitudes were used to minimize saturation of flowing ^{13}C-labelled molecules [5]. Imaging was performed on a GE 3T system using a adiabatic double spin-echo sequence with TE = 155ms, TR = 250ms, 10 Hz spectral resolution, 581 Hz spectra bandwidth, 12x12x16 matrix, 5x5x5.4 mm resolution, and 2 s per image. The sequence was started immediately following the 12 sec injection of a 350 uL solution containing 80 mM [1-^{13}C]-pyruvate and 80 mM ^{13}C-urea.

The curves were adjusted to account for the flip angle variations between metabolites by normalizing to $\sin(\theta)\cos^{Nflip}(\theta)$ after Nflip excitations. The "Mean Time" was calculated as the first moment of the dynamic curves to reflect the average arrival time. Also calculated were the Area Under Curve– reflecting total signal – and Full-width half-maximum (FWHM) – reflecting the wash-out rate.

Results:

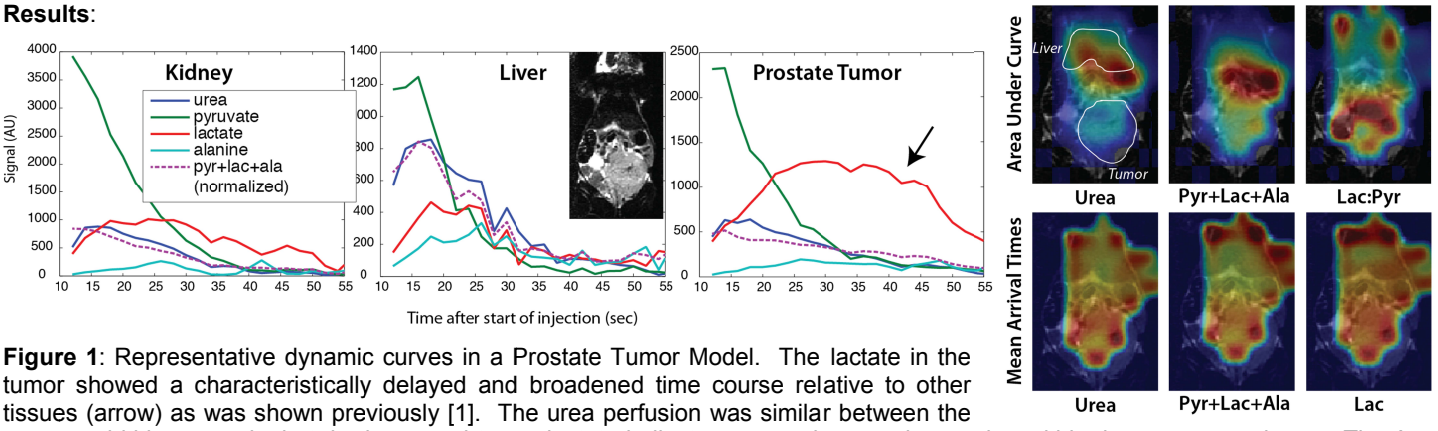

Figure 1: Representative dynamic curves in a Prostate Tumor Model. The lactate in the tumor showed a characteristically delayed and broadened time course relative to other tissues (arrow) as was shown previously [1]. The urea perfusion was similar between the tumor and kidney voxels, but the increased tumor lactate indicates conversion was happening within the cancerous tissue. The Area Under Curve maps (red = larger, green = smaller) show regional variations between urea and pyr+lac+ala, particularly in the liver and gut. The mean time maps (red = later, green = earlier) had very similar distributions, and a later arrival in the tumor than in the liver.

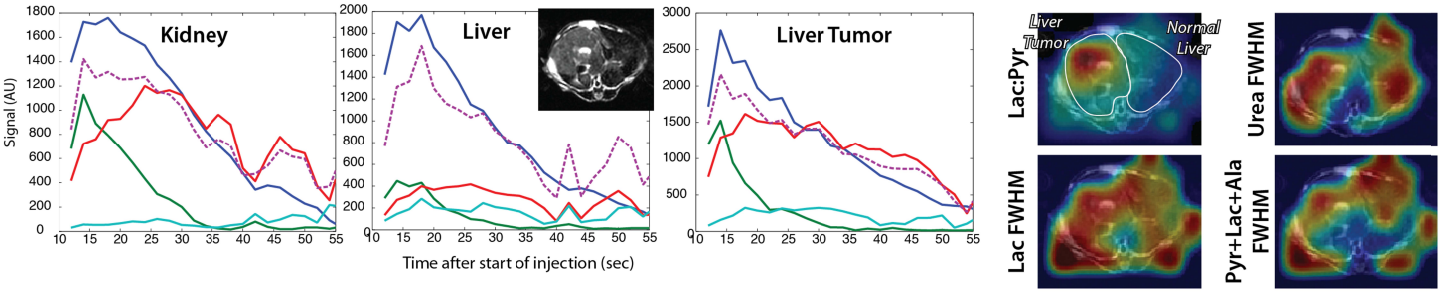

Figure 2: Representative dynamic curves in a Liver Tumor Model. The relative urea polarization was larger in this study than in Fig. 1. The tumor had characteristically high lactate [6], while the urea and pyr+lac+ala curves showed similar variations in time. In this study, the tumor had greater lactate to pyruvate and lactate to urea than the other voxels, reflecting the higher rate of metabolic conversion. The FWHM maps show rapid wash-out near the major vessels, and generally longer retention in the peripheral tumor regions

Conclusions: Dynamic MRSI with copolarized [1-^{13}C]-pyruvate and ^{13}C-urea allows for simultaneous assessment of perfusion and metabolism. This also leads to improved separation of perfusing metabolites from those generated within metabolically active tissues.

References: [1] Larson et al. MRM, 63:582-591, 2010. [2] Wilson et al. JMR 205: 141–147, 2010. [3] Von Morze et al, JMRI 33: 692-697, 2011. [4] Larson, et al. MRM, 65:610–619, 2011. [5] Josan et al, JMR, 209: 332-336, 2011. [6] Hu et al. Cell Metabolism, 14: 131-142, 2011. *Support from NIH P41EB013598 and R00 EB012064*